

A generalized configuration model with triadic closure

Ruhui Zhang, Duan-Shin Lee, *Member, IEEE*, and Cheng-Shang Chang, *Fellow, IEEE*

Abstract—In this paper we present a generalized configuration model with random triadic closure (GCTC). This model possesses five fundamental properties: large clustering coefficient, power law degree distribution, short path length, non-zero Pearson degree correlation, and existence of community structures. We analytically derive the Pearson degree correlation coefficient and the clustering coefficient of the proposed model. We select a few datasets of real-world networks. By simulation, we show that the GCTC model matches very well with the datasets in terms of Pearson degree correlations and clustering coefficients. We also test three well-known community detection algorithms on our model, the datasets and other three prevalent benchmark models. We show that the GCTC model performs equally well as the other three benchmark models. Finally, we perform influence diffusion on the GCTC model using the independent cascade model and the linear threshold model. We show that the influence spreads of the GCTC model are much closer to those of the datasets than the other benchmark models. This suggests that the GCTC model is a suitable tool to study network science problems where degree correlation or clustering plays an important role.

Index Terms—configuration model, degree correlation, clustering coefficient, community detection, influence diffusion

1 INTRODUCTION

NETWORK science is an inter-disciplinary field that formulates research problems arising in science and engineering into problems in graphs. To study successfully these diversified problems, researchers need suitable graph models. It would be nice to have a random graph model that possesses a rich set of topological properties and can be used to study a wide variety of problems in network science. In the mean time, it would be nice that the random graph model is simple enough to allow mathematical studies. There are five properties that are commonly observed in many real-life networks in science and engineering [1], [2]. They are

- 1) large clustering coefficient;
- 2) short average path length;
- 3) scale-free degree distribution, *i.e.* power law distribution;
- 4) assortative or disassortative degree correlation, and
- 5) existence of community structures.

In this paper we propose a random network model that possesses the five properties above. Many research problems in network science tie closely with these five properties. For instance, it is well known that diseases transmit efficiently among people in densely connected clusters, such as members in a household [3], [4]. It is also well known that clustering affects significantly the resilience of a network [5]. It is also commonly observed that densely connected clusters affect significantly how opinions spread in a network

[6], [7]. To study these problems, one needs a graph model that is rich in transitivity. Authors in [8], [9], [10] showed that degree correlations and power law degree distributions have strong influence to the threshold of an epidemic. To study epidemic or influence diffusion problems, one may need a graph model that possesses degree correlations. The purpose of this paper is to propose a random graph model that is suitable to be used to study a broad range of problems. Our random model has all the five properties listed in the previous paragraph and is simple enough to allow mathematical analysis. It has a rich set of parameters and allows users to match its degree distribution, clustering coefficient, and degree correlation with those of a real-world dataset.

Our proposed model is based on configuration models originally proposed by Bender [11]. A configuration model is defined and constructed for a given degree sequence. It can have a power law degree distribution, if the given degree sequence is drawn from a power law distribution. It possesses a small world property. However, it lacks a community structure, and its clustering coefficient and degree correlation are asymptotically small as the network grows in size. Lee *et al.* [12] proposed a generalized configuration model, which adds a positive or a negative degree correlation to the configuration model. Lee *et al.* [12] achieved a non-zero degree correlation by partitioning stubs of edges into blocks and connecting stubs according to certain rules. In this paper, we propose to add another layer of blocks to emulate an artificial structure of communities. The result is a random graph model that possesses the fifth property listed in the first paragraph of this section. In addition, we propose to add triangles into the model to create a significant clustering coefficient. In literature, there are several proposals to achieve this objective. We refer the reader to [13], [14] and the references therein. In this paper we propose to add triangles by performing triadic closure

• Ruhui Zhang is with the Department of Computer Science, and Duan-Shin Lee is with the Department of Computer Science and the Institute of Communications Engineering, and Cheng-Shang Chang is with the Institute of Communications Engineering, National Tsing Hua University, Hsinchu 300, Taiwan, R.O.C. (Email: hui@cs.nthu.edu.tw; lds@cs.nthu.edu.tw; cschang@ee.nthu.edu.tw)

This research was supported in part by the Ministry of Science and Technology, Taiwan, R.O.C., under Contract 109-2221-E-007-093-MY2.

operations [15], [16]. In social science, triadic closure means that there is an increased likelihood that two people, who have a friend in common, will become friends [15]. Triadic closure has been observed in many real-world networks. For instance, Kossinets and Watts found clear evidence of triadic closure by taking multiple snapshots on an email communication network using a dataset consisting of 22,000 students at a large U.S. university [17]. Moreover, Leskovec *et al.* [18] analyzed the properties of triadic closure in online social networks of LinkedIn, Flickr, Del.icio.us, and Yahoo! Answers. In this paper we propose a random triadic closure operation. That is, all connected triples that are not triangles yet are closed and become triangles with some probabilities. With these two new features, the new model possesses large transitivity and community structures. We call the new model generalized configuration model with triadic closure (GCTC). The detail construction algorithm of the GCTC model will be presented in Section 2. We mention some research work in the literature that is related to triadic closure. Zhou *et al.* [19] proposed a network embedding method that takes the status of triads into consideration. Their method can learn representation vector for each vertex at different time points. Hofstad *et al.* [20] used term “triadic closure” to refer to triangles in a network. Hofstad *et al.* studied configuration models with power law degree distributions. Specifically, they showed that the local clustering coefficient of vertices with degree k and network size n is of the order $n^{5-2\tau}k^{-2(3-\tau)}$ for $\tau \in (2, 3)$, where τ is the exponent of the power law degree distribution [20]. Clustering coefficients have been a widely accepted metric to measure triadic closure. Yin *et al.* [21] proposed new metrics to measure triadic closure in directed graphs.

We now outline the contributions of this paper. First, we derive closed form expressions for the Pearson degree correlation coefficient and the clustering coefficient of the new proposed GCTC model. We mention that there are other proposals of random networks that possess the five fundamental properties listed above. For example, Toivonen *et al.* [2] proposed a growth model that possesses all the five properties. It is not clear if the Pearson degree correlation coefficient of this model is mathematically tractable. Second, we examine whether the GCTC network is a suitable model to study various research problems in network science. We choose four datasets of networks collected in the real world. To make a comparison, we choose three random network models that are often used as benchmark models to evaluate community detection algorithms. The three models are stochastic blockmodel (SBM) [22], [23], Lancichinetti-Fortunato-Radicchi benchmark (LFR) model [24], [25] and artificial benchmark for community detection (ABCD) model [26]. Through simulations, we show that by choosing parameters properly the GCTC model can match better with the datasets in terms of the Pearson degree correlations and the clustering coefficients than the SBM, the LFR model and the ABCD model. Further, we compare the GCTC model with the SBM, the LFR model and the ABCD model using three well known community detection algorithms. We show that the GCTC model performs equally well as the other three benchmark models for community detection. Finally, we study influence diffusion in real-world networks, the GCTC model, the SBM, LFR

and ABCD models. We study this problem using both an independent cascade (IC) model [27], [28] and a linear threshold (LT) model [27], [29]. We find that the fraction of influenced nodes observed in the GCTC model is much closer to that of the real-world datasets, compared with the fraction corresponding to the SBM model, LFR, and the ABCD models. This implies that the GCTC network is a more suitable model to study the influence diffusion problem. These results seem to indicate that degree correlation and clustering coefficient are less relevant to the community detection problem, but are crucial to the influence diffusion problem.

The organization of this paper is as follows. In Section 2, we present a construction algorithm for the GCTC model. Then, we briefly review several basic analytical results of the generalized configuration model in Section 3. In Section 4 we analyze the Pearson degree correlation coefficient of the GCTC model. In Section 5 we analyze the clustering coefficient of the GCTC model. In Section 6 we present numerical and simulation results. Finally, we present the conclusions of this paper in Section 7.

2 CONSTRUCTION ALGORITHM

In this section we present a construction algorithm for the GCTC model. Recall that in a standard configuration model, two ends of an edge are called “stubs”. To construct a standard configuration model, an unconnected stub is connected to another randomly selected stub among all unconnected stubs [30]. This construction algorithm creates a random network that has asymptotically vanishing Pearson degree correlation coefficient as the network becomes large. To introduce non-zero Pearson degree correlation, Lee *et al.* [12] partition stubs into blocks according to vertex degrees. To introduce positive (resp. negative) correlation, the selected permutation function associates blocks of large (resp. small) degrees with another block of large (resp. small) degrees. Stubs in block i are designated into type 1 stubs and type 2 stubs. An unconnected type 1 stub in block i is connected to a randomly selected unconnected type 1 stub in the associated block of block i . An unconnected type 2 stub is connected to an unconnected type 2 stub randomly selected in *all* blocks. The construction algorithm of GCTC model is similar to that of a generalized configuration model, except that it has *two* additional features. First, GCTC model has two layers of blocks. Stubs are divided into macroscopic blocks, which model communities. In each macroscopic block, stubs are further divided into microscopic blocks, which are used to create a non-zero Pearson degree correlation. To achieve this, each stub is designated to one of *three* types. Type 1 and type 2 stubs provide intra-community connections and the non-zero degree correlation. Type 3 stubs provide intra-community as well as inter-community connections.

We describe the construction algorithm of GCTC model in details. There are c communities, where $c \geq 1$. Community i , where $i = 1, 2, \dots, c$, has n_i vertices. Let n be the total number of vertices in the network. It follows that

$$n = \sum_{i=1}^c n_i.$$

We note that the size of different communities can be distinct. That is, it is possible that $n_i \neq n_j$ for some $i \neq j$. Denote k_{ij} as the degree of the j -th vertex in community i . Define m_i such that

$$2m_i = \sum_{j=1}^{n_i} k_{ij}. \quad (1)$$

The quantity $2m_i$ in (1) is the total number of stubs attached to vertices in community i . The total number of edges in the network is m , where

$$m = \sum_{i=1}^c m_i.$$

For each community i , the edges are connected in the following ways. A degree k vertex in community i has k_i stubs. In this community i , we arrange the stubs associated with the vertices in an ascending order of the vertex degrees. We then partition the stubs into b_i blocks evenly. That is, each block has the same number of stubs. Denote block b_{ij} as the block j in community i . To create degree-degree correlations, we select a permutation function $h_i(b_{ij})$ for block b_{ij} . Specifically, block b_{ij} is associated with block b_{ii} , if $h_i(b_{ij}) = b_{ii}$. In addition, h_i is selected such that $h_i(h_i(b_{ij})) = b_{ij}$. We then classify the stubs in each block into three types proportionally. Denote the ratio of type 1 and type 2 stubs to the total stubs in each block in community i as $r_i \in [0, 1]$ and the ratio of type 1 stubs to the type 1 and type 2 stubs in each block in community i as $q_i \in [0, 1]$. Suppose r_i and q_i are given. For block b_{ij} , randomly designate $\lceil 2m_i q_i r_i / b_i \rceil$ stubs as type 1 stubs, and randomly designate $\lceil 2m_i (1 - q_i) r_i / b_i \rceil$ stubs as type 2 stubs. Designate the rest stubs in block b_{ij} as type 3 stubs. To make a connection, one randomly picks an unconnected stub, say stub s . If s is a type 1 stub in block b_{ij} of community i , connect it with a randomly selected unconnected type 1 stub in block $h_i(b_{ij})$ and connect it to s . If s is a type 2 stub, randomly select an unconnected type 2 stub in community i and connect it to s . If s is a type 3 stub, randomly select an unconnected type 3 stub in the network and connect the stub to s . These edges are referred to as *regular edges*.

Next, we apply triadic closure operations to increase the number of triangles in the network. The edges added into the network by the triadic closure operations are called *transitive edges*. We examine all pairs of unconnected vertices in the network. For each pair of unconnected vertices, say vertices A and B , if A and B have d common neighbors, we connect A and B with probability a_d . With probability $1 - a_d$, A and B remain unconnected. The construction algorithm for the GCTC model is shown in Algorithm 1.

3 REVIEW OF THE GENERALIZED CONFIGURATION MODEL

In this section we review some basic results of the generalized configuration model in [12]. These results will be used to derive Pearson degree correlation coefficient of the GCTC model in Section 4 and the clustering coefficient of the GCTC model in Section 5. We note that the generalized configuration model is a special case of the GCTC model where $c = 1$, $r_1 = 1$ and $a_d = 0$. We drop subscripts and

Algorithm 1 Construction Algorithm

Inputs: Degree sequence $\{k_{ij} : i = 1, 2, \dots, c, j = 1, 2, \dots, n_i\}$, parameters $\{b_i : i = 1, 2, \dots, c\}$, $\{q_i : i = 1, 2, \dots, c\}$, $\{r_i : i = 1, 2, \dots, c\}$, $\{h_i : i = 1, 2, \dots, c\}$ and $\{a_d : d = 1, 2, \dots, n - 2\}$.

Outputs: graph $G = (V, E)$

```

1: for  $i = 1, 2, \dots, c$  do
2:   For community  $i$ , create  $2m_i$  stubs from degree sequence  $\{k_{ij} : j = 1, 2, \dots, n_i\}$  and arrange the stubs in an ascending order according to the degrees;
3:   Divide  $2m_i$  stubs into  $b_i$  blocks evenly;
4:   for  $j = 1, 2, \dots, b_i$  do
5:     For block  $j$  of community  $i$ , randomly designate  $\lceil 2m_i q_i r_i / b_i \rceil$  stubs as type 1 stubs, and randomly designate  $\lceil 2m_i (1 - q_i) r_i / b_i \rceil$  stubs as type 2 stubs;
6:     Designate rest stubs in block  $j$  as type 3 stubs;
7:   end for
8: end for
9: while there are unconnected stubs do
10:  Randomly select a stub. Assume that the stub is in block  $j$  of community  $i$ ;
11:  if type 1 stub then
12:    connect this stub with a randomly selected type 1 unconnected stub in block  $h_i(j)$  in community  $i$ ;
13:  else if type 2 stub then
14:    connect this stub with a randomly selected type 2 unconnected stub in community  $i$ ;
15:  else
16:    connect this stub with a randomly selected type 3 stub among all type 3 stubs that are unconnected in the network;
17:  end if
18: end while
19: for each unconnected pair of vertices do
20:   if these two vertices have  $d$  common neighbors then
21:     with probability  $a_d$ , these two vertices are connected with a transitive edge, and with probability  $1 - a_d$  leave these two vertices unconnected;
22:   end if
23: end for

```

use notation b , q , and $h(i)$ to denote the number of blocks, the fraction of type 1 stubs, and the permutation function of block i , respectively.

Let Z be the degree of a randomly selected vertex in the generalized configuration network. Then, the pmf of Z is $\{p_k\}$ and

$$\mathbb{E}[Z] = \sum_{k=0}^{\infty} k p_k. \quad (2)$$

The following assumption is crucial to the analysis. This assumption is stringent. We refer readers to [12] for additional information on this assumption.

Assumption 1. The degree distribution $\{p_k\}$ is said to satisfy this assumption if one can find mutually disjoint sets H_1, H_2, \dots, H_b , such that

$$\bigcup_{i=1}^b H_i = \{0, 1, 2, \dots\}$$

and

$$\sum_{k \in H_i} kp_k = \mathbb{E}[Z]/b \quad (3)$$

for all $i = 1, 2, \dots, b$. In addition, we assume that the degree sequence k_1, k_2, \dots, k_n sampled from the distribution $\{p_k\}$ can be evenly placed in b blocks. That is, each block has the same number of stubs. In addition, stubs that belong to vertices of the same degrees are placed in the same block. Mathematically speaking, there exist mutually disjoint sets H_1, H_2, \dots, H_b that satisfy

- 1) $\bigcup_{i=1}^b H_i = \{1, 2, \dots, n\}$,
- 2) $k_i \neq k_j$ for any $i \in H_{\ell_1}, j \in H_{\ell_2}, \ell_1 \neq \ell_2$, and
- 3) $\sum_{j \in H_i} k_j = 2m/b$ for all $i = 1, 2, \dots, b$.

We randomly select a stub in the range $[1, 2m]$. Denote this stub by t . Let v be the vertex, with which stub t is associated. Let Y be the degree of vertex v . Since the stub is randomly selected and vertices with degree y have $ny p_y$ stubs. We have

$$\Pr(Y = y) = \frac{ny p_y}{2m} = \frac{y p_y}{\mathbb{E}[Z]}. \quad (4)$$

Now connect stub t to a randomly selected stub. Let this stub be denoted by s . Let u be the vertex, with which s is associated, and let X be the degree of vertex u . Next we study $\Pr(X = x|Y = y)$. We assume that Assumption 1 holds. Suppose x is a degree in set H_i . The total number of stubs which are associated with vertices with degree x is $n x p_x$. By Assumption 1, all $n x p_x$ stubs are in block i . There are two cases, in which stub t connects to stub s . In the first case, stub t is of type 1. This occurs with probability q . In this case, stub s must be a type 1 stub and belong to a vertex with a degree in block $h(i)$. With probability

$$\frac{q n x p_x}{2m q/b - \delta_{i,h(i)}}, \quad (5)$$

the construction algorithm in Section 2 connects t to stub s . In (5) $\delta_{i,j}$ is the Kronecker delta, is equal to one if $i = j$, and is equal to zero otherwise. In the second case, stub t is of type 2. This occurs with probability $1 - q$. In this case, stub s can be associated with a degree in any block. With probability

$$\frac{(1 - q) n x p_x}{2m(1 - q) - 1} \quad (6)$$

the construction algorithm connects stub t to stub s . Combining the two cases in (5) and (6), we have

$$\Pr(X = x|Y = y) = \frac{q^2 n x p_x}{2m q/b - \delta_{i,h(i)}} + \frac{(1 - q)^2 n x p_x}{2m(1 - q) - 1} \quad (7)$$

for $y \in H_{h(i)}$. If $y \in H_j$ for $j \neq h(i)$,

$$\Pr(X = x|Y = y) = \frac{(1 - q)^2 n x p_x}{2m(1 - q) - 1}. \quad (8)$$

Now assume that the network is large. That is, we consider a sequence of constructed graphs, in which $n \rightarrow \infty, m \rightarrow \infty$, while keeping $2m/n = \mathbb{E}[Z]$. Under this asymptotic, Eqs. (7) and (8) converge to

$$\Pr(X = x|Y = y) \rightarrow \begin{cases} \frac{qb + (1 - q)}{\mathbb{E}[Z]^2} x p_x, & y \in H_{h(i)} \\ \frac{1 - q}{\mathbb{E}[Z]^2} x p_x, & y \in H_j, j \neq h(i). \end{cases} \quad (9)$$

From (4) and (9) we obtain

$$\begin{aligned} \Pr(X = x, Y = y) &= \Pr(X = x|Y = y)\Pr(Y = y) \\ &= \begin{cases} \frac{qb + (1 - q)}{(\mathbb{E}[Z])^2} x y p_x p_y, & x \in H_i, y \in H_{h(i)} \\ \frac{1 - q}{(\mathbb{E}[Z])^2} x y p_x p_y, & x \in H_i, y \in H_j, j \neq h(i) \end{cases} \end{aligned} \quad (10)$$

We next analyze the expected value of Y and the product XY , respectively. From (4), we obtain

$$\mathbb{E}[Y] = \sum_y y \Pr(Y = y) = \sum_{j=1}^b \sum_{y \in H_j} \frac{y^2 p_y}{\mathbb{E}[Z]} = \frac{1}{\mathbb{E}[Z]} \sum_{j=1}^b u_j. \quad (11)$$

where

$$u_j = \sum_{y \in H_j} y^2 p_y. \quad (12)$$

From (10), we have

$$\begin{aligned} \mathbb{E}[XY] &= \sum_x \sum_y x y \Pr(X = x, Y = y) \\ &= \frac{1 - q}{(\mathbb{E}[Z])^2} \sum_{i=1}^b \sum_{j=1}^b u_i u_j + \frac{qb}{(\mathbb{E}[Z])^2} \sum_{i=1}^b u_i u_{h(i)}. \end{aligned} \quad (13)$$

We now consider $\mathbb{E}[Y|X]$. Denote the conditional expectation $\mathbb{E}[Y|X = x]$ by $g(x)$. Assume that $x \in H_i$ for some i . From (9), we have

$$\begin{aligned} g(x) &= \mathbb{E}[Y|X = x] \\ &= \sum_{i=1}^b \frac{(1 - q) u_i}{\mathbb{E}[Z]} + \frac{q b u_{h(i)}}{\mathbb{E}[Z]}. \end{aligned} \quad (14)$$

In addition, the analysis of the clustering coefficient needs the probability that two specific vertices are connected by a regular edge. Randomly select two vertices, say vertices A and B . Denote the degrees of A and B by X_A and X_B . Let the blocks of A and B be Q_A, Q_B , respectively. We now consider the conditional connection probability

$$\begin{aligned} p_c(A, B) &= \\ \Pr(\text{vertices } A \text{ and } B \text{ are connected} | X_A = k_A, X_B = k_B, \\ &\quad Q_A = i, Q_B = j). \end{aligned} \quad (15)$$

If $h(i) \neq j$, vertices A and B can only be connected through a pair of type 2 stubs. A type 2 stub of vertex A connects to a type 2 stub of vertex B with probability $(1 - q)k_B/(2m(1 - q))$, since B has on average $(1 - q)k_B$ type 2 stubs, there are totally $2m(1 - q)$ type 2 stubs in the network, and the connection is randomly selected. Since vertex A has $(1 - q)k_A$ type 2 stubs on average, it follows that

$$p_c(A, B) = \frac{(1 - q)^2 k_A k_B}{2m(1 - q)} = \frac{(1 - q) k_A k_B}{2m}. \quad (16)$$

If $h(i) = j$, vertices A and B can be connected through a pair of type 1 or type 2 stubs. In this case,

$$p_c(A, B) = \frac{(1 - q)^2 k_A k_B}{2m(1 - q)} + \frac{q^2 k_A k_B}{2m q/b} = \frac{(1 - q + qb) k_A k_B}{2m}. \quad (17)$$

4 PEARSON DEGREE CORRELATION COEFFICIENT

In the section we analyze the Pearson degree correlation of the GCTC model. Recall that the GCTC model can have multiple communities. Stubs corresponding to vertices are first divided into communities. In each community, stubs are divided into blocks to create a non-zero Pearson degree correlation. This two layer structure of stubs does not change the mathematical nature on how Pearson degree correlation being derived. However, it does increase the number of cases and the complexity of notations significantly. For this reason, we assume that there is one community in this section. In this special case, $c = 1$, $r_i = 1$, $h_i(i) = h(i)$ and $a_d = a$.

Pearson degree correlation is defined as the Pearson correlation coefficient of degrees at the two ends of a randomly selected edge. The GCTC model has two types of edges, regular edges and transitive edges. In this paper we analyze the correlation coefficient of degrees at the two ends of a randomly selected regular edge. Randomly select an edge among regular edges in the network. Let X and Y be the number of regular edges that the two ends of the edge have. Let X' and Y' be the number of transitive edges that the two ends of the edge have. We shall analyze the Pearson degree correlation

$$\rho(X + X', Y + Y') \stackrel{\text{def}}{=} \frac{\text{Cov}(X + X', Y + Y')}{\sigma_{X+X'}\sigma_{Y+Y'}} \quad (18)$$

where $\text{Cov}(X + X', Y + Y')$ is the co-variance of random variables $X + X'$ and $Y + Y'$ and $\sigma_{X+X'}$ is the standard deviation of $X + X'$.

Recall that in the generalized configuration model, the degree covariance is defined as $\text{Cov}(X, Y) = E[XY] - E[X]E[Y]$ and $\sigma_X = E[X^2] - (E[X])^2$. In the GCTC model, the degree co-variance is defined as

$$\begin{aligned} \text{Cov}(X + X', Y + Y') &= (E[XY] - E[X]E[Y]) + (E[X'Y] - E[X']E[Y]) \\ &\quad + (E[XY'] - E[X]E[Y']) + (E[X'Y'] - E[X']E[Y']). \end{aligned} \quad (19)$$

And the product of standard deviations in the denominator of (18) is equal to

$$\begin{aligned} \sigma_{X+X'}\sigma_{Y+Y'} &= \sigma_{X+X'}^2 \\ &= E[X^2] - (E[X])^2 + 2(E[XX'] - E[X]E[X']) \\ &\quad + E[(X')^2] - (E[X'])^2. \end{aligned} \quad (20)$$

Compared with $\text{Cov}(X, Y)$, $\text{Cov}(X + X', Y + Y')$ has additional expected terms related to X' and Y' . Before we present the derivations of $E[X']$, $E[X'Y]$ and $E[X'Y']$, we first show the following theorem. It is one of the main results in this paper. Its proof is presented in Appendix B at the end of this paper.

Theorem 2. If $h(i) = i$, then

$$\text{Cov}(X + X', Y + Y') \geq \text{Cov}(X, Y) \geq 0. \quad (21)$$

We next analyze the terms needed to compute $\text{Cov}(X + X', Y + Y')$ and $\sigma_{X+X'}$. We observe that all the quantities of these expected terms are in the form of $E[X^i Y^j (E[Y|X])^k (E[X|Y])^l]$ for some integers i, j, k and l . Therefore, we present the analysis of $\text{Cov}(X + X', Y + Y')$

in the following three subsections. In Section 4.1, we show the analysis of $E[X']$, $E[X'Y]$ and $E[X'Y']$. We next analyze the expected value $E[X^i Y^j (E[Y|X])^k (E[X|Y])^l]$ for integers i, j, k and l in Section 4.2. In Section 4.3, we present the final equations of $\text{Cov}(X + X', Y + Y')$. Since the analysis of $\sigma_{X+X'}$ is similar to $\text{Cov}(X + X', Y + Y')$, we present the analysis of $\sigma_{X+X'}$ in Appendix-C.

4.1 Analysis of $E[X']$, $E[X'Y]$, and $E[X'Y']$

To analyze $E[X']$, $E[X'Y]$, and $E[X'Y']$, we shall first analyze the expected value of X' . Recall that X and Y are the number of regular edges that two vertices at the two ends of a randomly selected regular edge. Let A and B denote the two vertices. X' and Y' are the number of transitive edges that A and B have, respectively. Number the X regular edges such that the first edge connects to B . Along the i -th regular edge of A to reach the other side, where $i = 2, 3, \dots, X$, one finds Y_i regular edges. A graphical illustration is shown in Figure 1.

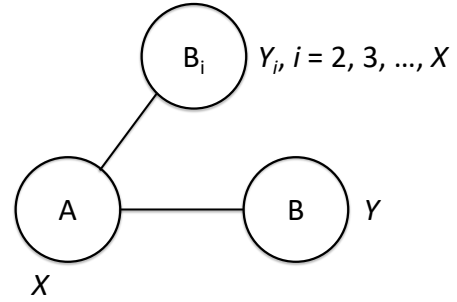


Fig. 1: Edge AB is a randomly selected regular edge. Vertex A has X regular edges. The first edge connects to B , which has Y regular edges. The i -th edge connects to vertex B_i , which has Y_i regular edges.

Along the first edge, A has $Y - 1$ second neighbors and along the i -th edge, A has $Y_i - 1$ second neighbors. Totally, vertex A has

$$Y - 1 + \sum_{i=2}^X (Y_i - 1) \quad (22)$$

second neighbors. The total number of second neighbors in (22) can be overestimated, as some second neighbors can be counted more than once. However, as the network size is large, the error is asymptotically small. We also remark that random variables Y_i , $i \leq 2$, are identically distributed for large networks. Their common distribution is the same as that of Y . The number of transitive edges that vertex A has, given X and Y , is

$$X' = \sum_{j=1}^{Y-1} B_{1,j} + \sum_{i=2}^X \sum_{j=1}^{Y_i-1} B_{i,j}, \quad (23)$$

where $\{B_{ij} : i \geq 1, j \geq 1\}$ is a doubly indexed sequence of independent and identically distributed Bernoulli random

variables with success probability a . The conditional expectation of X' , given X and Y , is

$$\begin{aligned} \mathbb{E}[X'|X, Y] &= \mathbb{E} \left[\sum_{j=1}^{Y-1} B_{1,j} + \sum_{i=2}^X \sum_{j=1}^{Y_i-1} B_{ij} \middle| X, Y \right] \\ &= a \cdot (Y-1) + \sum_{i=2}^X a \cdot \mathbb{E}[Y_i - 1 | X]. \end{aligned} \quad (24)$$

Since Y_i and Y are identically distributed for all i , the preceding equation can be rewritten as

$$\mathbb{E}[X'|X, Y] = a(Y-1 + (X-1)\mathbb{E}[Y|X] - (X-1)). \quad (25)$$

Taking expectation with respect to X and Y , we have

$$\begin{aligned} \mathbb{E}[X'] &= a(\mathbb{E}[Y] - 1 + \mathbb{E}[XY] - \mathbb{E}[Y] - \mathbb{E}[X] + 1) \\ &= a(\mathbb{E}[XY] - \mathbb{E}[X]). \end{aligned} \quad (26)$$

Next, we analyze $\mathbb{E}[X'Y]$. From (23) and similar to (24), we have

$$\begin{aligned} \mathbb{E}[X'Y|X, Y] &= \mathbb{E} \left[\left(\sum_{j=1}^{Y-1} B_{1,j} + \sum_{i=2}^X \sum_{j=1}^{Y_i-1} B_{ij} \right) Y \middle| X, Y \right] \\ &= a((Y-1)Y + (X-1)Y \cdot \mathbb{E}[Y-1|X]) \\ &= a(Y^2 - XY + XY\mathbb{E}[Y|X] - Y\mathbb{E}[Y|X]). \end{aligned}$$

It follows that

$$\mathbb{E}[X'Y] = a(\mathbb{E}[Y^2] - \mathbb{E}[XY] + \mathbb{E}[XY\mathbb{E}[Y|X]] - \mathbb{E}[Y\mathbb{E}[Y|X]]). \quad (27)$$

We see that the terms on the right of the preceding expression are in the form of $\mathbb{E}[X^i Y^j (\mathbb{E}[Y|X])^k (\mathbb{E}[X|Y])^l]$ for some integers i, j, k and l . We shall analyze these terms in the next subsection.

Finally, we analyze $\mathbb{E}[X'Y']$. From (23), we have

$$\begin{aligned} \mathbb{E}[X'Y'|X, Y] &= \mathbb{E} \left[\left(\sum_{j=1}^{Y-1} B_{1,j} + \sum_{i=2}^X \sum_{j=1}^{Y_i-1} B_{ij} \right) \cdot \left(\sum_{j=1}^{X-1} C_{1,j} + \sum_{i=2}^Y \sum_{j=1}^{X_i-1} C_{ij} \right) \middle| X, Y \right], \end{aligned}$$

where $\{C_{ij} : i \geq 1, j \geq 1\}$ is a doubly indexed sequence of independent and identically distributed Bernoulli random variables with success probability a . Doubly indexed sequences $\{B_{ij}\}$ and $\{C_{ij}\}$ are independent. Thus, we have

$$\begin{aligned} \mathbb{E}[X'Y'|X, Y] &= a^2(Y-1 + (X-1)\mathbb{E}[Y|X] - (X-1)) \\ &\quad \cdot (X-1 + (Y-1)\mathbb{E}[X|Y] - (Y-1)). \end{aligned}$$

Then, we obtain

$$\begin{aligned} \mathbb{E}[X'Y'] &= a^2(-2\mathbb{E}[X^2] + 2\mathbb{E}[X^2Y] \\ &\quad - 2\mathbb{E}[XY\mathbb{E}[Y|X]] + 2\mathbb{E}[Y\mathbb{E}[Y|X]] \\ &\quad + \mathbb{E}[\mathbb{E}[Y|X]\mathbb{E}[X|Y]] \\ &\quad - 2\mathbb{E}[Y\mathbb{E}[Y|X]\mathbb{E}[X|Y]] \\ &\quad + \mathbb{E}[XY\mathbb{E}[Y|X]\mathbb{E}[X|Y]]). \end{aligned} \quad (28)$$

4.2 Analysis of $\mathbb{E}[X^i Y^j (\mathbb{E}[Y|X])^k (\mathbb{E}[X|Y])^l]$

We have observed that all quantities of expected values in (19) and (20) are in the form of $\mathbb{E}[X^i Y^j (\mathbb{E}[Y|X])^k (\mathbb{E}[X|Y])^l]$ for some integers i, j, k and l . Instead of tediously presenting the derivations of all expectation terms needed to compute the covariance and the variance, we choose a more complex term, that is $\mathbb{E}[X^2 (\mathbb{E}[Y|X])^2]$, and derive it in this subsection. The derivation of other terms is similar, and is omitted. We simply present the result in Appendix A.

With (14), we have

$$\begin{aligned} \mathbb{E}[X^2 (\mathbb{E}[Y|X])^2] &= \sum_x (xg(x))^2 \mathbb{P}(X=x) \\ &= \sum_{i=1}^b \sum_{x \in H_i} \left(\sum_{i=1}^b \frac{(1-q)u_i}{\mathbb{E}[Z]} + \frac{qb u_{h(i)}}{\mathbb{E}[Z]} \right)^2 \\ &\quad \cdot x^2 \cdot \frac{x p_x}{\mathbb{E}[Z]} \\ &= (1-q)^2 \frac{(\mathbb{E}[Z^2])^2 \mathbb{E}[Z^3]}{(\mathbb{E}[Z])^3} \\ &\quad + 2(1-q)qb \frac{\mathbb{E}[Z^2]}{(\mathbb{E}[Z])^3} \sum_{i=1}^b u_{h(i)} t_i \\ &\quad + q^2 b^2 \frac{1}{(\mathbb{E}[Z])^3} \sum_{i=1}^b (u_{h(i)})^2 t_i, \end{aligned}$$

where

$$t_i = \sum_{x \in H_i} x^3 p_x. \quad (29)$$

4.3 Analysis of $\text{Cov}(X + X', Y + Y')$

Finally, substituting (41), (26), (43), (27), and (28) into (19), we obtain

$$\text{Cov}(X + X', Y + Y') = \alpha_0 + \sum_{i=1}^5 \beta_i W_i, \quad (30)$$

where

$$\begin{aligned} \alpha_0 &= 2a \frac{a(\mathbb{E}[Z^2] - \mathbb{E}[Z]) + \mathbb{E}[Z]}{(\mathbb{E}[Z])^3} (\mathbb{E}[Z]\mathbb{E}[Z^3] - (\mathbb{E}[Z^2])^2) \\ \beta_1 &= \frac{q}{(\mathbb{E}[Z])^2} + 2a \frac{q}{(\mathbb{E}[Z])^2} \left(\frac{(1-q)\mathbb{E}[Z^2]}{\mathbb{E}[Z]} - 1 \right) \\ &\quad + a^2 \frac{q(((1-q)\mathbb{E}[Z^2] + q\mathbb{E}[Z])^2 - 2(2-q^2)\mathbb{E}[Z^2]\mathbb{E}[Z])}{(\mathbb{E}[Z])^4} \\ \beta_2 &= 2a^2 \frac{q}{(\mathbb{E}[Z])^2} \\ \beta_3 &= -2a \frac{q^2}{(\mathbb{E}[Z])^2} \left((1-a) + a \frac{(1-q)\mathbb{E}[Z^2]}{\mathbb{E}[Z]} \right) \\ \beta_4 &= 2a \frac{q^2 b}{(\mathbb{E}[Z])^3} \left((1-a) - aq + a \frac{(1-q)\mathbb{E}[Z^2]}{\mathbb{E}[Z]} \right) \\ \beta_5 &= a^2 \frac{q^3 b^2}{(\mathbb{E}[Z])^4} \end{aligned}$$

$$W_1 = b \sum_{i=1}^b u_i u_{h(i)} - \sum_{i=1}^b u_i \sum_{j=1}^b u_j \quad (31)$$

$$W_2 = b \sum_{i=1}^b t_i u_{h(i)} - \sum_{i=1}^b u_i \sum_{j=1}^b t_j \quad (32)$$

$$W_3 = b \sum_{i=1}^b u_i u_i - \sum_{i=1}^b u_i \sum_{j=1}^b u_j \quad (33)$$

$$W_4 = b \sum_{i=1}^b u_i u_{h(i)} u_i - \sum_{i=1}^b u_i u_{h(i)} \sum_{j=1}^b u_j \quad (34)$$

$$W_5 = b \sum_{i=1}^b u_i u_{h(i)} u_i u_{h(i)} - \sum_{i=1}^b u_i u_{h(i)} \sum_{j=1}^b u_j u_{h(j)}. \quad (35)$$

In (31) and (32), sequences $\{u_i\}$ and $\{t_i\}$ are defined in (12) and (29), respectively.

5 CLUSTERING COEFFICIENT

In this section we analyze the local clustering coefficient of the GCTC model. We remark that in this section we study the clustering coefficient of a special case in which there is only one community. We also remark that it is easy to extend the analysis to GCTC models with more than one community. We choose to present the result of the special case in order to keep notational simplicity.

Let A be a randomly selected vertex in a random network. Let k be the degree of A . The local clustering coefficient of vertex A is defined as

$$C_A(k) = \frac{\text{number of connected pairs of neighbors of } A}{\text{number of pairs of neighbors of } A} = \frac{\text{number of connected pairs of neighbors of } A}{k(k-1)/2}. \quad (36)$$

If $k \leq 1$, $C_A(k)$ is defined to be zero. We distinguish between regular edges and transitive edges. Assume that vertex A has k regular edges and k' transitive edges. We denote the local clustering coefficient of A by $C_A(k, k')$. Let the k vertices connected with A by regular edges be denoted by U_1, U_2, \dots, U_k . Let the k' vertices connected with A by transitive edges be denoted by $V_1, V_2, \dots, V_{k'}$.

We analyze the numerator of (36). Obviously, if $k = 0$, $C_A(0, k') = 0$. For general $k \geq 1$ and $k' \geq 0$, we claim that

$$C_A(k, k') = \frac{\binom{k}{2} a + k' + \binom{k'}{2} \times \frac{a}{k}}{\binom{k+k'}{2}}, \quad (37)$$

with the convention that

$$\binom{i}{j} = 0 \text{ if } i < j.$$

To analyze (37) we consider six types of triangles as shown in Figure 2. We consider type 1 triangles shown in panel (a) of Figure 2. The expected number of type 1 triangles is

$$\sum_{k_1, k_2} \binom{k}{2} p_c(U_1, U_2) p_{k_1} p_{k_2},$$

where k_1 and k_2 are the degrees of vertices U_1 and U_2 , respectively. Since $2m = nE[Z]$, it follows that the expected number of type 1 triangles in the last expression approaches to zero as the network size n is large. Note that type 5 triangles in panel (e) of Figure 2 also require vertices U_1 and U_2 be connected by regular edges. By the same argument, it

is easy to see that the expected number of type 5 triangles also goes to zero as the network gets large.

Now we consider the second type of triangles shown in panel (b) of Figure 2. Vertices U_1 and U_2 are connected by a transitive edge. This transitive edge is formed because vertex U_2 is an unconnected second neighbor of U_1 through vertex A . Thus, the expected number of type 2 triangles is

$$\sum_{k_1, k_2} \binom{k}{2} (1 - p_c(U_1, U_2) p_{k_1} p_{k_2}) \cdot a = \binom{k}{2} \cdot a.$$

This is the first term in the numerator of (37).

We next analyze type 3 triangles shown in panel (c) of Figure 2. Note that transitive edge AV_1 can be formed in two types of event. The first type of event is the successful event of random triadic closure of the connected triples of A , V_1 and U_1 . The second type of event is the successful event of random triadic closure of the connected triples of A , V_1 and one of the first neighbors of A in the set $\{U_1, U_2, \dots, U_k\}$ except U_1 . If the transitive edge AV_1 in type 3 triangle is formed from the first type of event, the number of type 3 is k' . If the transitive edge AV_1 is formed from the second type of event, to form a type 3 triangle, U_1 and V_1 need to be connected by a regular edge. From the analysis of type 1 triangles, we know that the connected probability of U_1 and V_1 approaches to zero as the network size n is large. To sum, the expected number of type 3 triangles is k' , which is the second term in the numerator of (37).

Now we consider type 4 triangles shown in panel (d) of Figure 2. In order to form a transitive edge between U_1 and V_1 , these two vertices must have at least one common neighbor by regular edges. Besides vertices A , U_1 and V_1 , there are $n-3$ vertices in the network. Let E_{n-3} be the event that there is at least one vertex in $n-3$ vertices that connects to both U_1 and V_1 . Then, the expected number of type 4 triangles is

$$kk'aP(E_{n-3}) = kk'a(1 - P(E_{n-3}^c)), \quad (38)$$

where E_{n-3}^c is the complement of event E_{n-3} . Denote the $n-3$ vertices by vertices $1, 2, \dots, n-3$.

$$P(E_{n-3}^c) = \sum_{u, v, k_1, k_2, \dots, k_{n-3}} \prod_{j=1}^{n-3} (1 - p_c(j, U_1))(1 - p_c(j, V_1)) \times p_u p_v p_{k_1} p_{k_2} \cdots p_{k_{n-3}}, \quad (39)$$

where u and v are the degrees of U_1 and V_1 , and k_j is the degree of vertex j for $j = 1, 2, \dots, n-3$. To evaluate $P(E_{n-3})$, we substitute (16) or (17) into (39). For example, denote b_{U_1} , b_{V_1} and b_j as the block index of U_1 , V_1 and j , respectively. Suppose $b_{U_1} \neq h(b_j)$ and $b_{V_1} \neq h(b_j)$, we substitute (16) into (39) and have

$$\begin{aligned} P(E_{n-3}) &= 1 - \sum_{u, v, k_1, k_2, \dots, k_{n-3}} \prod_{j=1}^{n-3} \prod_{j=1}^{n-3} \left(1 - \frac{(1-q)uk_j}{2m} \cdot \frac{(1-q)v(k_j-1)}{2m} \right) \\ &\quad \times p_u p_v p_{k_1} p_{k_2} \cdots p_{k_{n-3}} \\ &= 1 - \sum_{u, v} \left(1 - \frac{(1-q)^2 uv (E[Z^2] - E[Z])}{(nE[Z])^2} \right)^{n-3} p_u p_v \\ &\leq 1 - \left(1 - \frac{(1-q)^2 (E[Z])^2 (E[Z^2] - E[Z])}{(nE[Z])^2} \right)^{n-3} \end{aligned} \quad (40)$$

$\rightarrow 0$ as $n \rightarrow \infty$,

where inequality (40) is due to Jensen's inequality [31]. It follows that the expected number of type 4 triangles is zero in large networks. Note that substitution of (17) into (39) leads to the same result, *i.e.* the expected number of type 4 triangles is zero in large networks.

Finally, we consider the expected number of type 6 triangles shown in panel (f) of Figure 2. Note that to form transitive edges AV_1 and AV_2 , vertices V_1 and V_2 must be unconnected second neighbors of A through some first neighbors of A in the set $\{U_1, U_2, \dots, U_k\}$. There are two cases. In the first case shown in panel (a) of Figure 3, V_1 and V_2 have distinct common neighbors with A . Vertices V_1 and V_2 randomly and independently select first neighbors from the set $\{U_1, U_2, \dots, U_k\}$. The probability that their selections are distinct is

$$(k-1)/k.$$

Thus, the expected number of type 6 triangles in the first case is

$$\binom{k'}{2} \cdot \frac{k-1}{k} \cdot a \cdot P(E_{n-5}).$$

By the same argument in (40), it is easy to show that the quantity above goes to zero as n goes to infinity. Now we consider the second case shown panel (b) of Figure 3. Vertices V_1 and V_2 share a common first neighbor U_i with A . The probability that the random selections of V_1 and V_2 are the same is $1/k$. Thus, the expected number of type 6 triangles is

$$\binom{k'}{2} \cdot \frac{a}{k}.$$

This is the third term in the numerator on the right side of (37).

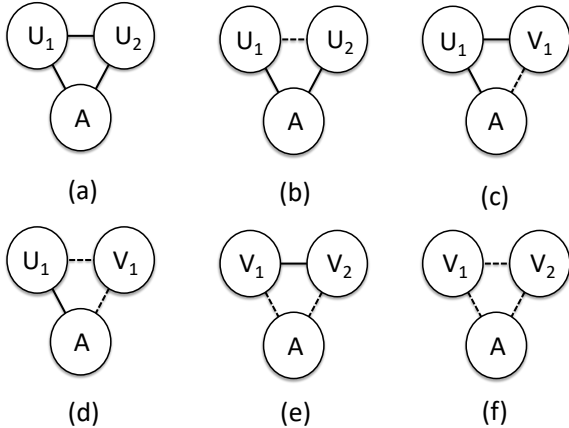


Fig. 2: Six types of triangles. Solid lines denote regular edges of the GCTC model. Dashed lines denote transitive edges due to triadic closure operations.

6 SIMULATION RESULTS

In this section we present our numerical and simulation results. We present our results in four subsections. First, since our closed form expressions for the Pearson degree

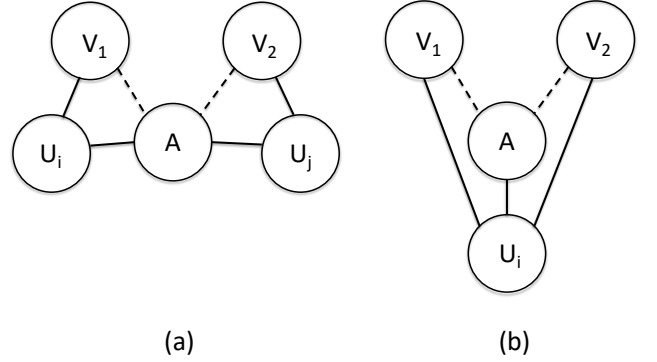


Fig. 3: Type 6 triangles. Vertices V_1 and V_2 must be unconnected second neighbors of A through some first neighbors U_i and U_j . In panel (a), the two first neighbors of A are distinct. In panel (b), vertices V_1 and V_2 have a common first neighbor of A .

correlation coefficient and the clustering coefficient are quite complicated, we verify their correctness by comparing numerical results with simulation results in Section 6.1. In Section 6.2 we model four real-world networks by GCTC networks. To make a comparison we also model the same real-world networks using SBM, LFR and ABCD models. In Section 6.3, we study whether the GCTC model is suitable to be a benchmark model for community detection algorithms. Finally, in Section 6.4 we simulate influence diffusion in GCTC networks and compare the result with that in a real-world network.

6.1 Correctness of Eqs. (30) and (37)

Since our closed form expressions in Eqs. (30) and (37) are quite complicated, we verify their correctness by comparing their numerical results with simulation results. Recall that we assume $c = 1$, *i.e.* there is only one community in the derivation of Pearson degree correlation coefficient and clustering coefficient in Sections 4 and 5. We drop subscripts and use notations b and q to denote the number of blocks and the fraction of type 1 stubs. In our experiment, we assume that there are 10000 vertices. We sample a power law degree distribution to generate one degree sequence. For this degree sequence, we randomly construct fifty GCTC networks. We calculate the Pearson degree correlation coefficients and the clustering coefficients of the fifty networks and take an average. We choose $b = 2$.

We first consider positive degree correlation and assume that blocks are associated with each other by permutation $h(i) = i$. We present the numerical calculation and simulation of covariance $\text{Cov}(X + X', Y + Y')$ as a function of q in Figure 4. Then, we examine Pearson degree correlation coefficient $\rho(X + X', Y + Y')$ for permutation $h(i) = i$ and permutation $h(i) = b + 1 - i$. The result is shown in Figure 5. Note that without triadic closure operations permutation $h(i) = b + 1 - i$ would generate disassortatively mixed networks [12]. Figure 5 shows that with

triadic closure operations and small value of q , permutation $h(i) = b + 1 - i$ could generate assortatively mixed graphs. Finally, we notice that the numerical results agree very well with the simulation results in Figure 4 and Figure 5.

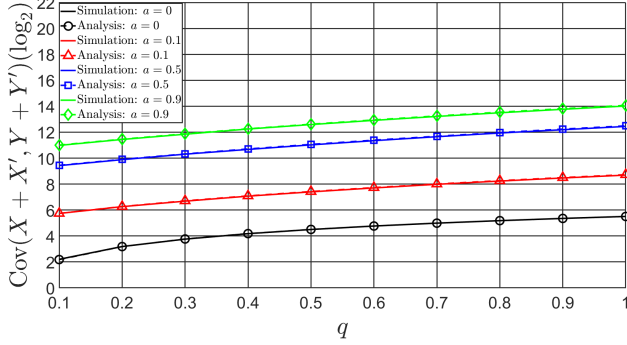


Fig. 4: Plot of co-variance versus q with $h(i) = i$.

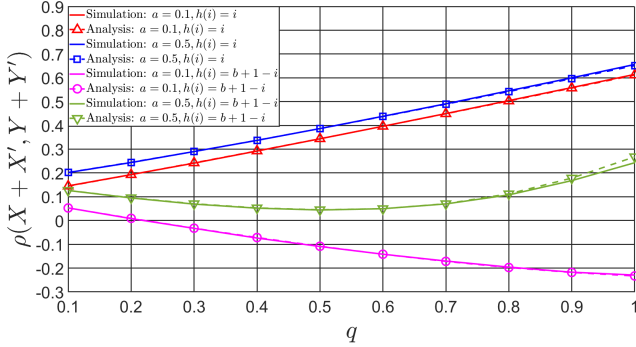


Fig. 5: Plot of Pearson degree correlation versus q .

Next, we numerically compute and simulate the clustering coefficient of the GCTC graph. The clustering coefficient is calculated by taking an average of the clustering coefficients of vertices in the network. The results are shown in Figure 6. We find that the simulation result and the numerical calculation of Eq. (37) are very close. We notice from Figure 6 that the clustering coefficient is increasing with a , which implies that triadic closure operations increase the transitivity of the network. We also notice that the range of clustering coefficient is somewhat narrow for a relatively wide range of a and q .

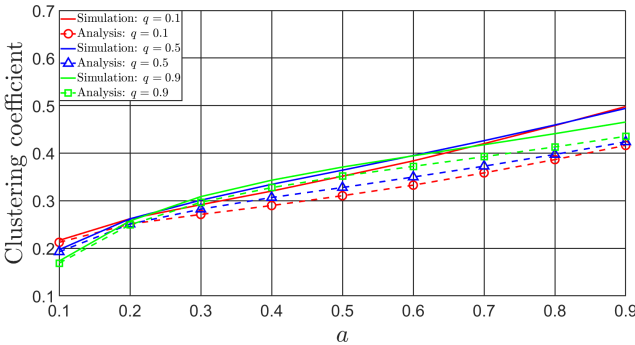


Fig. 6: Plot of clustering coefficient versus a with $h(i) = i$.

6.2 Modeling real-world networks

In this section we would like to study if it is possible to choose a proper set of parameters such that the degree

distribution, Pearson degree correlation coefficient and the clustering coefficient of the GCTC model match reasonably well with those of a real-life network. To study this problem, we choose four networks collected in the real life. Since we will study community detection algorithms on real-world networks in the next section, we choose real-world networks with a known community structure. Specifically, the four real-world networks that we choose are the Amazon network, the Email network, the Ogbn-arxiv network and the DBLP network. The Ogbn-arxiv data can be obtained from the OGB website¹. The other three network data are available at the Stanford website². These four datasets need pre-processing before they can be used. The Amazon network has multiple overlapped communities. We keep only one community and delete all other vertices. As a result, it has only one community. For the Email network, we keep communities with more than fifty vertices, and delete smaller communities. For the Ogbn-arxiv network, we only keep two largest communities whose sizes are smaller than ten thousand vertices. For the DBLP network, we keep the largest three communities.

We construct GCTC graphs with Algorithm 1 using properly selected parameters to match the performance of the four real-world graphs. The Pearson degree correlation coefficient, the clustering coefficient, the average length of shortest paths between randomly selected vertices, among others, are shown in Table 1. Note that due to triadic closure operations, the total number of edges m and the expected degree $E[Z]$ are not identically equal to those of the real-world networks. From column 7 and column 8, we see that the Pearson degree correlation coefficient and the clustering coefficient of the GCTC model match quite well with those of the four real-life networks.

To make a comparison, we also simulate three prevalent benchmark models that are often used to evaluate community detection algorithms. They are the SBM, the LFR model and the ABCD model. We briefly review these three models. The simplest SBM is a multi-graph with a given number of communities. Each vertex is assigned to a community. Undirected edges are placed independently between vertex pairs with probabilities that are only a function of the community membership of the vertices [22]. As a result, each vertex in an SBM has a Poisson distribution for its degree. To fit an SBM with an empirical network collected in the real world, one typically formulates a maximum likelihood problem to determine the parameters in the Poisson distributions. Unfortunately, the traditional SBM does not work well in the sense that it can not fit well with a wide range of network data. Karrer *et al.* [23] proposed a degree-corrected version of the SBMs. In the degree-corrected version, each vertex is associated with a new parameter, with which the parameters of Poisson distributions are multiplied and thus corrected. A maximum likelihood problem solves both the new parameters as well as the parameters of the Poisson distributions. We refer the reader to [23] for more details. In this paper, we choose the degree-corrected SBMs to fit with the four real-world networks. Next, we briefly review LFR model. An LFR graph is constructed first by sampling a power law

1. <https://ogb.stanford.edu/docs/nodeprop>
2. <https://snap.stanford.edu/data/>

distribution for a sequence of n degrees. Then a sequence of community sizes is sampled from another power law distribution. Clearly, the sum of all community sizes must be equal to the total number of vertices. Randomly assign each vertex to one community. Users of an LFR model also need to determine another parameter, the fraction of edges that connect two vertices in two distinct communities. Let μ denote this parameter. Each vertex is randomly connected by a fraction $1 - \mu$ of its links with vertices within its community and a fraction μ of its links with the other vertices of the network. Finally, we review ABCD model. The acronym ABCD stands for Artificial Benchmark for Community Detection. It is a modification of the LFR model in an attempt to make it be constructed faster. An ABCD model also has a parameter ξ called a mixing parameter. An ABCD model connects a fraction $1 - \xi$ of its edges to other vertices in the same community, and connects a fraction of ξ edges to vertices globally including the vertices in the same community. Finally, we mention that the construction algorithm for LFR networks has a complexity of $O(m^2)$. The construction algorithm for GCTC networks has a complexity of $O(n^3)$.

To model a given real-world network, we measure the fraction of edges connecting two vertices in two distinct communities. We call this quantity the mixing parameter of the real-world network. For simplicity, we set μ to this quantity and use it to construct LFR networks. We also use this quantity to calculate the value of ξ according to [26]. We then use ξ to construct ABCD networks. In Table 1, we present the values of the mixing parameter for the real-life networks and simulated graphs. Moreover, from the entries in columns 7 and 8 in Table 1, we see that the Pearson degree correlation coefficient and the clustering coefficient of the GCTC model match consistently better with those of the real-world networks than the SBM, the LFR model, and the ABCD model.

6.3 Community detection

One of the possible applications of the GCTC model is to serve as a benchmark model for community detection algorithms. In this section we compare the performance of the GCTC model with three well known benchmark models.

We test the performance of the GCTC model as a benchmark model using three well known community detection algorithms. They are the walktrap algorithm [32], the leading eigenvector algorithm [33] and the fast greedy algorithm [34]. We use normalized mutual information (NMI) to measure the performance of a benchmark model. We briefly state the definition of NMI here and refer the reader to [23], [35] for more details. Let n_{ij} be the number of vertices in community i in the inferred community detection and in community j in the ground truth. Define joint probability $\Pr(C_1 = i, C_2 = j) = n_{ij}/n$ that a randomly selected vertex is in i in the inferred detection and j in the ground truth. Using this joint probability over the random variables C_1 and C_2 , the NMI is defined as

$$NMI(C_1, C_2) = \frac{2MI(C_1, C_2)}{H(C_1) + H(C_2)},$$

where $MI(C_1, C_2)$ is the mutual information between C_1 and C_2 , $H(C_1)$ is the entropy of random variable C_1 , and

$H(C_2)$ is the entropy of random variable C_2 . Higher values of NMI indicate a higher degree of consistency between the detected structure of communities and the ground truth. Since the Amazon network has only one community, we have not applied community detection algorithms on it. For each benchmark model, we simulate and generate one thousand graphs. For each graph, we apply the three community detection algorithms and compute the NMI values. We present the average of the NMI values in columns 10, 11 and 12 in Table 1. From our simulation results, we see that the GCTC model performs better than the SBM, the LFR model, and the ABCD benchmark model when they model the Ogbn-arxiv network. For the other two real-world networks with leading eigenvector algorithm, the performance of the GCTC model is not the best. In fact, the performance of the GCTC model was the worst among the four benchmark models when the four models synthesize the Email network to evaluate the leading eigenvector algorithm. Since the NMI values of the GCTC model generally agree with those of the real-world networks and the other three random network models, we conclude that the GCTC model can serve well as a benchmark model for the evaluation of community detection algorithms. In addition, since the GCTC model performs the best in matching its ρ and C with those of the real-world networks, this study seems to imply that community detection problem is less sensitive to degree correlation and transitivity of a network. We observe that the mixing parameter for the DBLP network is very close to $1/2$. This fact might make the DBLP network very difficult for all community detection algorithms. Indeed, the NMI values of all the three community detection algorithms are very small.

6.4 Influence diffusion

We simulate influence cascade in the four real-world networks, the GCTC, the SBM, the LFR and the ABCD networks. We present results in this section.

We simulate two most prevalent influence cascade models, the IC model and the LT model [28]. In both models, the state of a vertex can be either active or inactive at any time step. Initially at time zero, a certain number of vertices are selected to be active. They are called the seeds of the diffusion. In the independent cascade model, when an inactive vertex becomes activated, it will independently activate each of its currently inactive neighbors with probability p in the next time step. Each active vertex has exactly one opportunity to influence its currently inactive neighbors. In our experiment, we set $p = 0.15$. In the linear threshold model, each inactive vertex, say v , computes the fraction of its active neighbors to its degree. The vertex switches to the active state if the fraction exceeds a threshold t . In the experiment we set $t = 0.35$. In both IC and LT models, the influence diffusion process unfolds in discrete time steps until no more vertices can be activated. We call the fraction of active vertices the influence spread of the diffusion process. This quantity is shown in columns **IC** and **LT**. From the entries in these two columns, we see that the GCTC model outperforms the other three models in predicting the influence spreads in both the IC model and the LT model in most cases. The only except is the

TABLE 1: Network properties of four real-world networks and four random graphs

Graph	n	m	$E[Z]$	c	mixing parameter	ρ	C	ℓ	Walktrap	Eigen	Fast	IC	LT
Amazon	310	895	5.77	1	0	-0.1239	0.4739	5.77	-	-	-	0.1867	0.2516
GCTC	310	861	5.55	1	0	-0.1122	0.5076	5.55	-	-	-	0.1323	0.2237
SBM	310	891	5.75	1	0	-0.0173	0.0300	3.33	-	-	-	0.2800	0.1581
LFR	310	895	5.77	1	0	-0.0169	0.0249	3.40	-	-	-	0.2634	0.1528
ABCD	310	895	5.77	1	0	-0.0169	0.0249	3.40	-	-	-	0.2634	0.1528
Email	225	1507	13.40	4	0.0902	-0.1025	0.4787	2.81	0.9300	0.8432	0.9166	0.6757	0.3467
GCTC	225	1535	13.64	4	0.0803	-0.0965	0.3895	2.77	0.9421	0.8943	0.9319	0.6991	0.3500
SBM	225	1442	12.82	4	0.0947	-0.0428	0.3500	2.72	0.8883	0.8353	0.8840	0.6525	0.3456
LFR	225	1507	13.40	4	0.1058	-0.1436	0.3789	2.64	0.9489	0.8757	0.9451	0.6970	0.3510
ABCD	225	1507	13.40	4	0.1056	-0.1445	0.3797	2.64	0.9490	0.8724	0.9446	0.6969	0.3504
Ogbn-arxiv	11315	32694	5.78	2	0.0138	0.0922	0.2508	7.50	0.2326	0.3053	0.3255	0.2191	0.4517
GCTC	11315	33256	5.88	2	0.0159	0.1019	0.2110	5.87	0.2534	0.3552	0.3569	0.2548	0.4343
SBM	11315	32693	5.78	2	0.0138	0.0131	0.0041	4.92	0.4636	0.3855	0.3798	0.3021	0.0506
LFR	11315	32726	5.78	2	0.0143	-0.0072	0.0040	5.08	0.4435	0.7323	0.4821	0.3005	0.0795
ABCD	11315	32728	5.78	2	0.0164	-0.0035	0.0041	5.05	0.4306	0.7605	0.4715	0.3006	0.0793
DBLP	15957	42943	5.38	3	0.4780	0.2038	0.6278	7.75	0.0674	0.0018	0.0201	0.1199	0.0315
GCTC	15957	42374	5.31	3	0.4659	0.2241	0.5232	9.56	0.0681	0.0097	0.0158	0.1205	0.0485
SBM	15957	42934	5.38	3	0.4782	0.0113	0.0012	4.92	0.1231	0.0489	0.0415	0.2782	0.0538
LFR	15957	42963	5.39	3	0.4783	-0.0014	0.0011	5.12	0.0963	0.0019	0.0016	0.2482	0.0647
ABCD	15957	42963	5.39	3	0.4848	-0.0011	0.0011	5.12	0.0953	0.0018	0.0016	0.2482	0.0656

In this table, n is the total number of vertices and m is the number of edges. $E[Z] = 2m/n$ is the average degree. The number of communities is c . The mixing parameter is the ratio of the number of edges cross communities to total number of the edges. Next, ρ is the Pearson degree correlation coefficient and C is the average of the local clustering coefficients of all vertices in the network. The average length of the shortest paths between two randomly selected vertices is ℓ . The entries in columns **Walktrap**, **Eigen**, and **Fast** are the NMI values of the walktrap, leading eigenvector and the fast greedy algorithms, respectively. The entries in columns **IC** and **LT** are the influence spread of the influence diffusion processes. We choose $p = 0.15$ as the probability of influence in the IC model. We choose $t = 0.35$ as the threshold in the LT model. In the IC model, we simulate the diffusion 1000 times on each graph and take an average. In both cascade models, we randomly select ten vertices as seeds in the largest communities in the Amazon network and in the Email network. We randomly select 100 and 200 vertices as seeds in the Ogbn-arxiv network and in the DBLP network, respectively. For the entries in columns ρ , C , ℓ , **Walktrap**, **Eigen**, **Fast**, **IC** and **LT**, we show in boldface those entries that are closest to the corresponding entries for real-world networks.

Email network. In both the independent cascade model and the linear threshold model, the influence spreads of the four random network models are very close. GCTC is not the worst among the four models. Studies in [6], [7] show that densely connected clusters affect significantly how opinions diffuse in a network. Recall that the degree correlations and transitivity of the GCTC model have the best match with those of real-world networks. It seems to imply that the influence diffusion problem is quite sensitive to the degree correlation and the clustering coefficient of the network in which the influence diffuses. In Figure 7 and Figure 8 we present the influence spread in the DBLP network and the four random network models as functions of p and t , respectively. From these two figures, we see that the influence spread of the real network can be very different from those in random networks for certain range of p and t . However, the curves corresponding to the GCTC model trace closely with those of the real network.

7 CONCLUSIONS

In this paper, we have presented a generalized configuration model with triadic closure. This model is an extension of the generalized configuration model by adding an additional layer of blocks and random triadic closure operations. The GCTC model possesses five most important properties of graphs that arise in network science. We have analyzed the Pearson degree correlation and clustering coefficient of

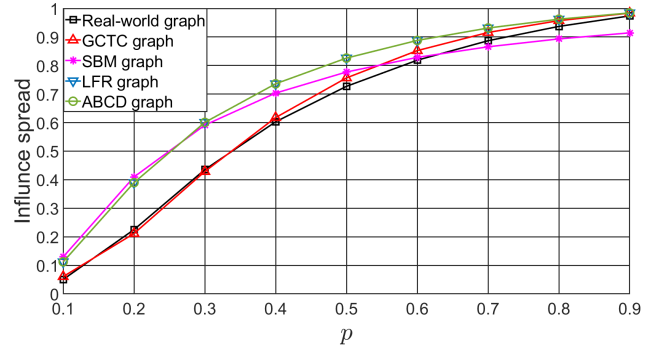


Fig. 7: Influence spread of the IC model on DBLP network

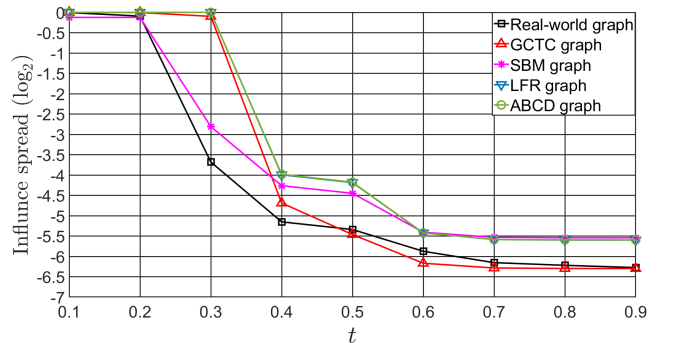


Fig. 8: Influence spread of the LT model on DBLP network

the GCTC model. We have applied the GCTC model, the SBM, the LFR model and the ABCD model to model four networks collected in the real world. We have shown that by choosing parameters properly the GCTC model matches much better its clustering coefficient and Pearson degree correlation coefficient with those of the data sets than the other three random models. We have used the GCTC model, the SBM, the LFR model, the ABCD model and the four real-world networks to examine three community detection algorithms and the influence diffusion problem. We found that the GCTC model, the SBM, the LFR model and the ABCD model perform nearly equally well as a benchmark model for community detection with GCTC model slightly better than the other three models. We have simulated influence diffusion in the four models and the four real-world networks using the independent cascade model and the linear threshold model. We found that the fraction of nodes influenced in the GCTC model matches much better with that of real-world networks than the other three models.

Appendix A

In this appendix we list all expectations needed to compute the covariance in Eq. (19) and the variance in Eq. (20). Note that $E[X]$ and $E[XY]$ have been derived in [12]. We repeat them here for easy reference.

$$E[X] = \frac{E[Z^2]}{E[Z]} \quad (41)$$

$$E[X^2] = \frac{E[Z^3]}{E[Z]} \quad (42)$$

$$E[XY] = \frac{1-q}{(E[Z])^2} \sum_{i=1}^b \sum_{j=1}^b u_i u_j + \frac{qb}{(E[Z])^2} \sum_{i=1}^b u_i u_{h(i)} \quad (43)$$

$$\begin{aligned} E[XY^2] &= E[X^2Y] \\ &= E[X^2E[Y|X]] \\ &= \frac{(1-q)E[Z^2]E[Z^3]}{(E[Z])^2} \\ &\quad + \frac{qb}{(E[Z])^2} \sum_{i=1}^b u_i t_{h(i)} \end{aligned} \quad (44)$$

$$E[XE[Y|X]] = E[YE[X|Y]] = E[XY] \quad (45)$$

$$\begin{aligned} E[YE[Y|X]] &= E[XE[X|Y]] \\ &= E[(E[Y|X])^2] \\ &= \frac{(1-q^2)(E[Z^2])^2}{(E[Z])^2} \\ &\quad + \frac{q^2b}{(E[Z])^2} \sum_{i=1}^b u_i u_i \end{aligned} \quad (46)$$

$$\begin{aligned} E[X(E[Y|X])^2] &= \frac{(1-q)^2(E[Z^2])^3}{(E[Z])^3} \\ &\quad + \frac{2(1-q)qbE[Z^2]}{(E[Z])^3} \sum_{i=1}^b u_i u_{h(i)} \\ &\quad + \frac{q^2b^2}{(E[Z])^3} \sum_{i=1}^b u_i u_{h(i)} u_{h(i)} \end{aligned} \quad (47)$$

$$\begin{aligned} E[X^2(E[Y|X])^2] &= (1-q)^2 \frac{(E[Z^2])^2 E[Z^3]}{(E[Z])^3} \\ &\quad + 2(1-q)qb \frac{E[Z^2]}{(E[Z])^3} \sum_{i=1}^b u_i t_{h(i)} \\ &\quad + q^2b^2 \frac{1}{(E[Z])^3} \sum_{i=1}^b (u_i)^2 t_{h(i)} \end{aligned} \quad (48)$$

$$\begin{aligned} E[XYE[Y|X]] &= E[XYE[X|Y]] \\ &= \frac{(1-q)^2(E[Z^2])^3}{(E[Z])^3} \\ &\quad + \frac{2(1-q)qbE[Z^2]}{(E[Z])^3} \sum_{i=1}^b u_i u_{h(i)} \\ &\quad + \frac{q^2b^2}{(E[Z])^3} \sum_{i=1}^b u_i u_{h(i)} u_{h(i)} \end{aligned} \quad (49)$$

$$\begin{aligned} E[E[Y|X]E[X|Y]] &= \frac{(1-q)(1+q+q^2)(E[Z^2])^2}{(E[Z])^2} \\ &\quad + \frac{q^3b}{(E[Z])^2} \sum_{i=1}^b u_i u_{h(i)} \end{aligned} \quad (50)$$

$$\begin{aligned} E[YE[Y|X]E[X|Y]] &= \frac{(1+q)(1-q)^2(E[Z^2])^3}{(E[Z])^3} \\ &\quad + \frac{(1-q^2)qbE[Z^2]}{(E[Z])^3} \sum_{i=1}^b u_i u_{h(i)} \\ &\quad + \frac{(1-q)q^2bE[Z^2]}{(E[Z])^3} \sum_{i=1}^b u_i u_i \\ &\quad + \frac{q^3b^2}{(E[Z])^3} \sum_{i=1}^b u_i u_i u_{h(i)} \end{aligned} \quad (51)$$

$$\begin{aligned} E[XYE[Y|X]E[X|Y]] &= \frac{(1-q)^3(E[Z^2])^4}{(E[Z])^4} \\ &\quad + \frac{3qb(1-q)^2(E[Z^2])^2}{(E[Z])^4} \sum_{i=1}^b u_i u_{h(i)} \\ &\quad + \frac{q^2b^2(1-q)}{(E[Z])^4} \left(\sum_{i=1}^b u_i u_{h(i)} \right)^2 \\ &\quad + \frac{2q^2b^2(1-q)E[Z^2]}{(E[Z])^4} \sum_{i=1}^b u_i u_i u_{h(i)} \\ &\quad + \frac{q^3b^3}{(E[Z])^4} \sum_{i=1}^b u_i u_i u_{h(i)} u_{h(i)} \end{aligned} \quad (52)$$

Appendix B

In Appendix B, we present the proof of Theorem 2. Recall that stubs corresponding to the degrees are partitioned *evenly* into b blocks. Recall also that our construction algorithm arranges degrees in ascending order (descending order will also work). That is,

$$x \leq y \text{ for all } x \in H_i \text{ and } y \in H_j,$$

where $i \leq j$. Due to Assumption 1, (3) holds. We break down the proof of Theorem 2 into several lemmas listed as follows.

Lemma 3. Suppose that $h(i) = i$. If sequences $\{x_i, i = 1, 2, \dots, b\}$ and $\{y_i, i = 1, 2, \dots, b\}$ are both non-decreasing or both non-increasing, then

$$b \sum_{i=1}^b x_i y_{h(i)} - \sum_{i=1}^b x_i \sum_{j=1}^b y_j \geq 0. \quad (53)$$

Proof of Lemma 3. If sequences $\{x_i\}$ and $\{y_i\}$ are both non-increasing, then

$$x_{[i]} = x_i$$

$$y_{[i]} = y_i,$$

where $x_{[i]}$ denotes the i -th largest element in sequence $\{x_i\}$. On the other hand, if sequences $\{x_i\}$ and $\{y_i\}$ are both non-decreasing, then

$$x_{[i]} = x_{b-i+1}$$

$$y_{[i]} = y_{b-i+1}.$$

In either cases, we have

$$\sum_{i=1}^b x_i y_{h(i)} = \sum_{i=1}^b x_i y_i = \sum_{i=1}^b x_{[i]} y_{[i]}. \quad (54)$$

Now consider circular shift permutation $\sigma_j(\cdot)$ with $\sigma_j(i) = (i + j - 1 \bmod b) + 1$ for $j = 1, 2, \dots, b$. From symmetry, we have $\sigma_j(i) = \sigma_i(j)$. Thus,

$$\sum_{i=1}^b \sum_{j=1}^b x_i y_j = \sum_{i=1}^b \sum_{j=1}^b x_i y_{\sigma_i(j)} = \sum_{j=1}^b \sum_{i=1}^b x_i y_{\sigma_j(i)}. \quad (55)$$

Let

$$v_i = y_{\sigma_j(i)}.$$

Thus,

$$\sum_{i=1}^b x_i y_{\sigma_j(i)} = \sum_{i=1}^b x_i v_i \leq \sum_{i=1}^b x_{[i]} v_{[i]}. \quad (56)$$

The last inequality in (56) is due to the well known Hardy, Littlewood and Pólya rearrangement inequality (see e.g., the book [36], pp. 141). Clearly, sequence $\{v_i\}$ is a shifted version of $\{y_i\}$. Thus,

$$v_{[i]} = y_{[i]}.$$

Substituting the preceding equation and (56) into (55), we obtain

$$\sum_{i=1}^b \sum_{j=1}^b x_i y_j \leq \sum_{j=1}^b \sum_{i=1}^b x_{[i]} y_{[i]} = b \sum_{i=1}^b x_i y_i,$$

where the last equality in the preceding is due to (54). ■

Lemma 4. If stubs corresponding to degrees are arranged in ascending order evenly into blocks, then

- 1) $\{u_i : 1 \leq i \leq b\}$
- 2) $\{t_i : 1 \leq i \leq b\}$
- 3) $\{t_i - u_i : 1 \leq i \leq b\}$
- 4) $\{u_i^2 : 1 \leq i \leq b\}$
- 5) $\{u_i(u_i - c) : 1 \leq i \leq b\}$ for any constant c

are all non-decreasing sequences.

Proof of Lemma 4. Let i and j be two blocks, where $i < j$. From Assumption 1,

$$\sum_{x \in H_i} x p_x = \sum_{x \in H_j} x p_x. \quad (57)$$

Let x_i^{\max} denote the maximum degree in block i . Then,

$$\begin{aligned} u_i &= \sum_{x \in H_i} x^2 p_x \\ &\leq x_i^{\max} \sum_{x \in H_i} x p_x \\ &= x_i^{\max} \sum_{x \in H_j} x p_x \\ &\leq \sum_{x \in H_j} x^2 p_x \\ &= u_j. \end{aligned}$$

Other sequences can be proved similarly. ■

Lemma 5. If $h(i) = i$, then

$$W_i \geq 0$$

for $i = 1, 2, 3, 4, 5$.

Proof of Lemma 5. Lee *et al.* [12] proved that $W_1 \geq 0$ if $h(i) = i$. We now prove that $W_2 \geq 0$. From part 2 of Lemma 4, it follows that sequence $\{t_i : 1 \leq i \leq b\}$ is non-decreasing. It follows from Lemma 3 that $W_2 \geq 0$. Proof for $W_i \geq 0, 3 \leq i \leq 5$ is similar. ■

Lemma 6. If $h(i) = i$, then

$$W_2 \geq W_1.$$

Proof of Lemma 6. One can express

$$\begin{aligned} W_2 - W_1 &= b \sum_{i=1}^b u_i (t_{h(i)} - u_{h(i)}) - \sum_{i=1}^b \sum_{j=1}^b u_i (t_j - u_j) \\ &= b \sum_{i=1}^b u_i (t_i - u_i) - \sum_{i=1}^b \sum_{j=1}^b u_i (t_j - u_j). \end{aligned}$$

From part 3 of Lemma 4, it follows that sequence $\{t_i - u_i : 1 \leq i \leq b\}$ is non-decreasing. The claim of the lemma follows from Lemma 3. ■

Lemma 7. If $h(i) = i$, then

$$\mathbb{E}[Z] \mathbb{E}[Z^3] - (\mathbb{E}[Z^2])^2 \geq W_1 \quad (58)$$

$$W_4 - \frac{\mathbb{E}[Z]}{b} W_3 \geq 0 \quad (59)$$

Proof of Lemma 7. We first prove (58). Note that

$$\begin{aligned} &\mathbb{E}[Z^3] \mathbb{E}[Z] - (\mathbb{E}[Z^2])^2 - W_1 \\ &= b z \sum_{i=1}^b t_i - \left(\sum_{i=1}^b u_i \right)^2 - \left(b \sum_{i=1}^b u_i^2 - \sum_{i=1}^b u_i \sum_{j=1}^b u_j \right) \\ &= b \sum_{i=1}^b (t_i z - u_i^2), \end{aligned}$$

We claim that $t_i z \geq u_i^2$ for all i . Inequality (58) follows directly from this claim. We now prove the claim. From the definition of u_i and t_i in (12) and (29) respectively, we have

$$\begin{aligned}
t_i z - u_i^2 &= \sum_{x \in H_i} \sum_{y \in H_i} x^3 y p_x p_y - \sum_{x \in H_i} \sum_{y \in H_i} x^2 y^2 p_x p_y \\
&= \sum_{x \in H_i} \sum_{y \in H_i} x^2 y (x - y) p_x p_y \\
&= \sum_{x, y \in H_i, x > y} x^2 y (x - y) p_x p_y + \sum_{x, y \in H_i, x < y} x^2 y (x - y) p_x p_y \\
&= \sum_{x, y \in H_i, x > y} x^2 y (x - y) p_x p_y - \sum_{x, y \in H_i, x < y} x^2 y (y - x) p_x p_y \\
&= \sum_{x, y \in H_i, x > y} x^2 y (x - y) p_x p_y - \sum_{x, y \in H_i, y < x} y^2 x (x - y) p_y p_x,
\end{aligned}$$

where the last equality follows by exchanging symbols x and y in the second term of the last equation. The preceding difference equals

$$\sum_{x, y \in H_i, x > y} xy(x - y)^2 p_x p_y,$$

which is non-negative.

Next we prove (59). Note that $\frac{E[Z]}{b} = z \leq u_i$ for $i = 1, 2, \dots, b$. Substituting (33) and (34) into (59), we obtain

$$\begin{aligned}
W_4 - \frac{E[Z]}{b} W_3 &= \left(b \sum_{i=1}^b u_i u_i u_i - \sum_{i=1}^b u_i u_i \sum_{j=1}^b u_j \right) \\
&\quad - \left(b \sum_{i=1}^b u_i u_i z - \sum_{i=1}^b u_i z \sum_{j=1}^b u_j \right) \\
&= b \sum_{i=1}^b u_i u_i (u_i - z) - \sum_{i=1}^b u_i \sum_{j=1}^b u_j (u_j - z).
\end{aligned}$$

From part 3 of Lemma 4, it follows that sequence $\{u_i(u_i - z) : 1 \leq i \leq b\}$ is non-decreasing. Inequality (59) follows from Lemma 3. \blacksquare

Now we prove Theorem 2.

Proof of Theorem 2. Through extensive algebraic manipulation, we express the sum of the first three terms and the sum of the last three terms in (30) in a different manner, *i.e.*

$$\alpha_0 + \beta_1 W_1 + \beta_2 W_2 = D_1 + D_2 + D_3 + D_4 + D_5 \quad (60)$$

$$\beta_3 W_3 + \beta_4 W_4 + \beta_5 W_5 = D_6 + D_7, \quad (61)$$

where

$$D_1 = \frac{q}{(E[Z])^2} W_1 = \text{Cov}(X, Y) \quad (62)$$

$$\begin{aligned}
D_2 &= 2a^2 \frac{E[Z^2]}{(E[Z])^3} (E[Z]E[Z^3] - (E[Z^2])^2) \\
&\quad - 2a^2 q \frac{E[Z^2]}{(E[Z])^3} W_1 \\
&\quad + 2a \frac{q(1-q)E[Z^2]}{(E[Z])^3} W_1
\end{aligned}$$

$$- 2a^2 \frac{q(1-q)E[Z^2]}{(E[Z])^3} W_1 \quad (63)$$

$$\begin{aligned}
D_3 &= 2a(1-a) \frac{1}{(E[Z])^2} (E[Z]E[Z^3] - (E[Z^2])^2) \\
&\quad + 2a^2 \frac{q}{(E[Z])^2} W_2 - 2a \frac{q}{(E[Z])^2} W_1
\end{aligned} \quad (64)$$

$$D_4 = a^2 \frac{q(1-q)^2 (E[Z^2])^2}{(E[Z])^4} W_1 \quad (65)$$

$$D_5 = a^2 \frac{q^3}{(E[Z])^2} W_1 \quad (66)$$

$$\begin{aligned}
D_6 &= 2a \frac{q^2 b}{(E[Z])^3} \left(1 - a + \frac{(1-q)(E[Z^2])^2}{E[Z]} \right) \\
&\quad \times \left(W_4 - \frac{E[Z]}{b} W_3 \right)
\end{aligned} \quad (67)$$

$$D_7 = a^2 \frac{q^3 b^2}{(E[Z])^4} \left(W_5 - 2 \frac{E[Z]}{b} W_4 \right). \quad (68)$$

We claim that

$$D_i \geq 0, \quad i = 1, 2, 3, \dots, 7.$$

Since $D_1 = \text{Cov}(X, Y)$, the claim implies (21). In the rest of the proof, we focus on the proof of the claim.

From Lemma 5, $W_1 \geq 0$. It follows from (65) and (66) that $D_4 \geq 0$ and $D_5 \geq 0$. For D_2 , we place $E[Z]E[Z^3] - (E[Z^2])^2$ with W_1 and obtain a lower bound for D_2 , *i.e.*

$$D_2 \geq 2a(1-q)(a + (1-a)q) \frac{E[Z^2]}{(E[Z])^3} W_1,$$

which is greater than or equal to zero, because $W_1 \geq 0$.

Now we consider D_3 . We replace $E[Z]E[Z^3] - (E[Z^2])^2$ and W_2 with W_1 and obtain a lower bound for D_3 , *i.e.*

$$D_3 \geq 2a(1-a)(1-q) \frac{1}{(E[Z])^2} W_1,$$

which is greater than or equal to zero, again because $W_1 \geq 0$.

Now we analyze D_6 . From (67) it is clear that $D_6 \geq 0$, if and only if

$$W_4 - \frac{E[Z]}{b} W_3 \geq 0.$$

From (59) in Lemma 7, $W_4 - \frac{E[Z]}{b} W_3 \geq 0$ holds. Then, we have $D_6 \geq 0$.

Finally we analyze D_7 . From (68), $D_7 \geq 0$, if and only if

$$W_5 - 2 \frac{E[Z]}{b} W_4 \geq 0.$$

Replacing W_4 and W_5 with their definitions in (34) and (35), we have

$$\begin{aligned}
W_5 - 2 \frac{E[Z]}{b} W_4 &= \left(b \sum_{i=1}^b u_i u_i u_i u_i - \sum_{i=1}^b u_i u_i \sum_{j=1}^b u_j u_j \right) \\
&\quad - 2 \left(b \sum_{i=1}^b u_i u_i u_i z - \sum_{i=1}^b u_i u_i \sum_{j=1}^b u_j z \right) \\
&= b \sum_{i=1}^b u_i u_i u_i (u_i - 2z) - \sum_{i=1}^b u_i u_i \sum_{j=1}^b u_j (u_j - 2z). \quad (69)
\end{aligned}$$

From case (4) and case (5) of Lemma 4 and Lemma 3, it follows that the right side of (69) is non-negative. The proof of Theorem 2 is completed. ■

Appendix C

In Appendix C, we analyze $\sigma_{X+X'}$ in the denominator in Eq. (18). Among the expectation terms needed in the $\sigma_{X+X'}$, $E[X]$ and $E[X']$ were already analyzed. We next analyze $E[XX']$ and $E[(X')^2]$. Since Y_i and Y are identically distributed and $E[Y_i|X] = E[Y|X]$. From (23) we have

$$\begin{aligned} E[XX'] &= E[E[XX'|X, Y, Y_i, \forall i]] \\ &= E \left[E \left[X \left(\sum_{j=1}^{Y-1} B_{1,j} + \sum_{i=2}^X \sum_{j=1}^{Y_i-1} B_{ij} \right) \middle| X, Y, Y_i, \forall i \right] \right] \\ &= E \left[E \left[X \left(a(Y-1) + a \sum_{i=2}^X (Y_i-1) \right) \middle| X, Y, Y_i, \forall i \right] \right] \\ &= E[aX(E[Y|X] - 1 + (X-1)(E[Y|X] - 1))] \\ &= a(E[X^2Y] - E[X^2]). \end{aligned} \quad (70)$$

Next, we analyze $E[(X')^2]$. From (23), we have

$$\begin{aligned} E[(X')^2] &= E \left[E \left[\left(\sum_{j=1}^{Y-1} B_{1,j} + \sum_{i=2}^X \sum_{j=1}^{Y_i-1} B_{ij} \right)^2 \middle| X, Y, Y_i, \forall i \right] \right] \\ &= E \left[E \left[\left(\sum_{j=1}^{Y-1} B_{1,j} \right)^2 \middle| X, Y, Y_i, \forall i \right] \right] \\ &\quad + E \left[E \left[2 \left(\sum_{j=1}^{Y-1} B_{1,j} \right) \left(\sum_{i=2}^X \sum_{j=1}^{Y_i-1} B_{ij} \right) \middle| X, Y, Y_i, \forall i \right] \right] \\ &\quad + E \left[E \left[\left(\sum_{i=2}^X \sum_{j=1}^{Y_i-1} B_{ij} \right)^2 \middle| X, Y, Y_i, \forall i \right] \right]. \end{aligned} \quad (71)$$

The first term on the right side of Eq. (71) is equal to

$$\begin{aligned} &E \left[E \left[\sum_{i=1}^{Y-1} \sum_{j=1}^{Y-1} B_{1,i} B_{1,j} \middle| X, Y, Y_i, \forall i \right] \right] \\ &= E \left[E \left[\sum_{i=1}^{Y-1} B_{1,i}^2 + \sum_{i=1}^{Y-1} \sum_{\substack{j=1 \\ j \neq i}}^{Y-1} B_{1,i} B_{1,j} \middle| X, Y, Y_i, \forall i \right] \right] \\ &= a(E[Y] - 1) + a^2 E[(E[Y|X] - 1)(E[Y|X] - 2)] \\ &= a^2 E[(E[Y|X])^2] + (a - 3a^2)E[Y] + 2a^2 - a. \end{aligned}$$

The second term on the right side of Eq. (71) is equal to

$$\begin{aligned} &E \left[E \left[2 \left(\sum_{j=1}^{Y-1} B_{1,j} \right) \left(\sum_{i=2}^X \sum_{j=1}^{Y_i-1} B_{ij} \right) \middle| X, Y, Y_i, \forall i \right] \right] \\ &= E \left[E \left[2(Y-1) \cdot a^2 \cdot \left(\sum_{i=2}^X Y_i - (X-1) \right) \middle| X, Y, Y_i, \forall i \right] \right]. \end{aligned}$$

Taking average of the preceding with respect to Y_i for all i , while conditioning on X and Y , we have

$$\begin{aligned} &E \left[E \left[2 \left(\sum_{j=1}^{Y-1} B_{1,j} \right) \left(\sum_{i=2}^X \sum_{j=1}^{Y_i-1} B_{ij} \right) \middle| X, Y, Y_i, \forall i \right] \right] \\ &= 2a^2 E[(Y-1)(X-1)(E[Y|X] - 1)] \\ &= 2a^2 (-2E[XY] + 3E[X] + E[XYE[Y|X]] \\ &\quad - E[YE[Y|X]] - 1). \end{aligned}$$

Now consider the third term on the right of (71). It can be written as

$$\begin{aligned} &\left(\sum_{i=2}^X \sum_{j=1}^{Y_i-1} B_{ij} \right)^2 \\ &= \sum_{i=2}^X \sum_{j=1}^{Y_i-1} B_{i,j}^2 + \sum_{i=2}^X \sum_{j=1}^{Y_i-1} \sum_{\substack{k=2 \\ k \neq i}}^X \sum_{\ell=1}^{Y_k-1} B_{i,j} B_{k,\ell} \\ &\quad + \sum_{i=2}^X \sum_{j=1}^{Y_i-1} \sum_{\substack{\ell=1 \\ \ell \neq j}}^{Y_i-1} B_{i,j} B_{i,\ell}. \end{aligned} \quad (72)$$

The conditional expectation of (72), given X, Y and Y_i for all i , is

$$\begin{aligned} &a \sum_{i=2}^X (Y_i - 1) + a^2 \sum_{i=2}^X \sum_{\substack{k=2 \\ k \neq i}}^X (Y_i - 1)(Y_k - 1) \\ &\quad + a^2 \sum_{i=2}^X (Y_i - 1)(Y_i - 2). \end{aligned} \quad (73)$$

Taking average on (73) with respect to Y_i for all i , we have

$$\begin{aligned} &a(X-1)(E[Y|X] - 1) \\ &\quad + a^2(X-1)(X-2)E[(Y_2-1)(Y_3-1)|X]) \\ &\quad + a^2(X-1)E[(Y-1)(Y-2)|X]. \end{aligned}$$

Since Y_2 and Y_3 are conditional independent, given X , the preceding quantity is equal to

$$\begin{aligned} &a(X-1)(E[Y|X] - 1) \\ &\quad + a^2(X-1)(X-2)(E[Y|X] - 1)^2 \\ &\quad + a^2(X-1)E[(Y-1)(Y-2)|X]. \end{aligned} \quad (74)$$

Finally, taking average on (74) with respect to X , we obtain

$$\begin{aligned} &a(E[XY] - 2E[X] + 1) + \\ &\quad a^2(-E[X^2Y] + 3E[XY] - 2E[Y] \\ &\quad + E[X^2E[Y|X]E[Y|X]] \\ &\quad - 3E[XE[Y|X]E[Y|X]] \\ &\quad + 2E[E[Y|X]E[Y|X]]). \end{aligned} \quad (75)$$

This is the third term on the right side of (71).

REFERENCES

- [1] M. Newman, *Networks: An Introduction*. New York: Oxford University Press, 2010.
- [2] R. Toivonen, J.-P. Onnela, J. Saramäki, J. Hyvönen, and K. Kaski, "A model for social networks," *Physica A: Statistical Mechanics and its Applications*, vol. 371, no. 2, pp. 851–860, 2006.

- [3] E. Coupechoux and M. Lelarge, "How clustering affects epidemics in random networks," *Advances in Applied Probability*, vol. 46, no. 4, pp. 985–1008, 2014.
- [4] P. Trapman, "On analytical approaches to epidemics on networks," *Theoretical population biology*, vol. 71, no. 2, pp. 160–173, 2007.
- [5] J. P. Gleeson, S. Melnik, and A. Hackett, "How clustering affects the bond percolation threshold in complex networks," *Physical Review E*, vol. 81, no. 6, p. 066114, 2010.
- [6] S. Morris, "Contagion," *The Review of Economic Studies*, vol. 67, no. 1, pp. 57–78, 2000.
- [7] D. J. Watts and P. S. Dodds, "Networks, influence, and public opinion formation," *Journal of Consumer Research*, vol. 34, pp. 441 – 458, 2007.
- [8] M. Boguñá, R. Pastor-Satorras, and A. Vespignani, "Absence of epidemic threshold in scale-free networks with degree correlations," *Physical Review Letters*, vol. 90, p. 028701, 2003.
- [9] M. Boguñá and R. Pastor-Satorras, "Epidemic spreading in correlated complex networks," *Physical Review E*, vol. 66, p. 047104, 2002.
- [10] V. M. Eguíluz and K. Klemm, "Epidemic threshold in structured scale-free networks," *Physical Review Letters*, vol. 89, no. 10, 108701, 2002.
- [11] E. A. Bender and E. R. Canfield, "The asymptotic number of labelled graphs with given degree sequences," *J. Comb. Theory Series A*, vol. 24, pp. 296–307, 1978.
- [12] D.-S. Lee, C.-S. Chang, M. Zhu, and H.-C. Li, "A generalized configuration model with degree correlations and its percolation analysis," *Applied Network Science*, vol. 4, no. 1, p. 124, Dec 2019.
- [13] M. Newman, "Random graphs with clustering," *Physical review letters*, July 2009.
- [14] C. Wang, O. Lizardo, and D. Hachen, "Algorithms for generating large-scale clustered random graphs," *Network Science*, vol. 2, pp. 403–415, July 2014.
- [15] A. Rapoport, "Spread of information through a population with socio-structural bias i: Assumption of transitivity," *Bulletin of Mathematical Biophysics*, vol. 15, no. 4, pp. 523 – 533, 12 1953.
- [16] D. Easley and J. Kleinberg, *Networks, crowds and markets reasoning about a highly connected world*. Cambridge University Press, 2010.
- [17] G. Kossinets and D. J. Watts, "Empirical analysis of an evolving social network," *science*, vol. 311, no. 5757, pp. 88–90, 2006.
- [18] J. Leskovec, L. Backstrom, R. Kumar, and A. Tomkins, "Microscopic evolution of social networks," in *Proceedings of the 14th ACM SIGKDD international conference on Knowledge discovery and data mining*, 2008, pp. 462–470.
- [19] L. Zhou, Y. Yang, X. Ren, F. Wu, and Y. Zhuang, "Dynamic network embedding by modeling triadic closure process," *Proceedings of the AAAI Conference on Artificial Intelligence*, vol. 32, no. 1, Apr. 2018.
- [20] R. van der Hofstad, J. S. H. van Leeuwen, and C. Stegehuis, "Triadic closure in configuration models with unbounded degree fluctuations," *Journal of Statistical Physics*, vol. 173, no. 3–4, pp. 746–774, jan 2018.
- [21] H. Yin, A. R. Benson, and J. Ugander, "Measuring directed triadic closure with closure coefficients," *Network Science*, vol. 8, no. 4, pp. 551–573, jun 2020.
- [22] P. W. Holland, K. B. Laskey, and S. Leinhardt, "Stochastic block models: First steps," *Social Networks*, vol. 5, no. 2, pp. 109–137, 1983.
- [23] B. Karrer and M. E. J. Newman, "Stochastic blockmodels and community structure in networks," *Phys. Rev. E*, vol. 83, p. 016107, Jan 2011. [Online]. Available: <https://link.aps.org/doi/10.1103/PhysRevE.83.016107>
- [24] A. Lancichinetti, S. Fortunato, and F. Radicchi, "Benchmark graphs for testing community detection algorithms," *Physical review E*, vol. 78, no. 4, p. 046110, 2008.
- [25] A. Lancichinetti and S. Fortunato, "Benchmarks for testing community detection algorithms on directed and weighted graphs with overlapping communities," *Physical Review E*, vol. 80, no. 1, p. 016118, 2009.
- [26] B. Kamiński, P. Prałat, and F. Théberge, "Artificial benchmark for community detection (abcd)—fast random graph model with community structure," *Network Science*, p. 1–26, 2021.
- [27] D. Kempe, J. Kleinberg, and É. Tardos, "Maximizing the spread of influence through a social network," in *Proceedings of the ninth ACM SIGKDD international conference on Knowledge discovery and data mining*, 2003, pp. 137–146.
- [28] P. Shakaran, A. Bhatnagar, A. Aleali, E. Shaabani, and R. Guo, "The independent cascade and linear threshold models," in *Diffusion in Social Networks*. Springer, 2015, pp. 35–48.
- [29] A. Borodin, Y. Filmus, and J. Oren, "Threshold models for competitive influence in social networks," in *International workshop on internet and network economics*. Springer, 2010, pp. 539–550.
- [30] Béla Bollobás, "A probabilistic proof of an asymptotic formula for the number of labelled regular graphs," *European Journal of Combinatorics*, vol. 1, pp. 311–316, 1980.
- [31] W. Feller, *An Introduction to Probability Theory and Its Application*. New York: John Wiley & Sons Inc., 1971, vol. 1 and 2.
- [32] P. Pons and M. Latapy, "Computing communities in large networks using random walks," *ISCIS 2005*, pp. 284–293, 2005.
- [33] M. Newman, "Finding community structure in networks using the eigenvectors of matrices," *Phys. Rev. E*, vol. 74, no. 3, p. 036104, 2006.
- [34] A. Clauset, M. E. Newman, and C. Moore, "Finding community structure in very large networks," *Physical review E*, vol. 70, no. 6, p. 066111, 2004.
- [35] L. Danon, A. Díaz-Guilera, J. Duch, and A. Arenas, "Comparing community structure identification," *Journal of Statistical Mechanics: Theory and Experiment*, vol. 2005, p. P09008, 2005.
- [36] A. Marshall, I. Olkin, and B. C. Arnold, *Inequalities: Theory of Majorization and Its Applications*. New York: Springer, 2011.